J Surfact Deterg (2017) 20:623–630
DOI 10.1007/s11743-017-1955-7

ORIGINAL ARTICLE

Analysis of the Effects of Hydrocarbon Chain on Foam Properties of Alkyl Polyglycosides

Yawen Zhou[1] · Shan Wang[1] · Mengdie Lv[1] · Jinping Niu[2] · Baocai Xu[1]

Received: 25 September 2016 / Accepted: 17 March 2017 / Published online: 25 March 2017

Abstract The influence of surfactant structure on foam properties of different alkyl polyglycosides (APGs) in aqueous solutions was studied. Foamability, foam stability, and foam morphology were analyzed using the FoamScan method. Results showed that the foamability, foam stability, and the liquid carrying ability of long-chain APGs are higher than those of short-chain APGs. Foam morphology analysis showed that the foam produced by short-chain APGs is more unstable than the foam generated by long-chain APGs. Long-chain APGs have stronger intermolecular cohesion force, stringency, and ductility than short-chain APGs.

Keywords Foaming abilities · Foam morphology · Foam stability · FoamScan · Anionic surfactants

Introduction

Foams are thermodynamically unstable systems in which gas bubbles are separated by thin liquid films [1, 2]. The main mechanisms of foam destruction are liquid drainage, Ostwald ripening, and bubble coalescence [3]. Foams are widely used in a variety of applications, such as cosmetology, food processing, firefighting, foam rubbers, detergents, and enhanced oil recovery, because of their large specific surface area [4–8]. Foamability and foam stability are usually used to describe foaming behavior. Foamability describes the ability of a solution to produce foam and is evaluated by obtaining the time to produce a certain volume of foam or the volume of foam after blowing for a certain time [9]. Foam stability is commonly monitored by the foam volume or the liquid volume of the solution draining out of the foam as a function of time [10].

The nature of the surfactant and their molecular structure affect the properties of foam films [11, 12]. The relationship between foam properties and surfactant molecular structure has been reported. An extensive study using the foam pressure drop technique demonstrated the foam film's stability with increasing CnTAB hydrophobic chain [13]. Gemini surfactants were found to be better foam stabilizers than their corresponding alkyl monomers [14], and the effect of the increased length of alkyl tails on the foam stability is consistent with the effect of interfacial elasticity of the foam film [15]. Polyoxyethylene alkyl ether (n = 10, 12, 14, and 16) was studied by monitoring the dynamic surface tension and aqueous core thickness of a vertical foam film with FT-IR. Results showed that the foamability of polyoxyethylene alkyl ether decreases with increasing hydrophobicity or polarity of the surfactant molecule's end groups [16, 17]. The rigid linking group favors static foam stability but decreases dynamic foam stability, whereas the soft linking groups enhance dynamic foam stability [10]. Foam stability of branched-alkyl benzene sulfonates increases when the position of the substituted benzene ring is closer to the middle because of the increasing surface dilational elasticity and compactness of the surfactant monolayer [18]. The flexibility and entanglement of hydrophobic groups play an important role in

✉ Baocai Xu
xubac@163.com

[1] Institute of Food and Chemical Engineering, Beijing Technology and Business University, Beijing 100048, People's Republic of China

[2] China Research Institute of Daily Chemical Industry, 34 # Wenyuan Str., Taiyuan 030001, Shanxi Province, People's Republic of China

surface dilational elasticity and in the strength of surface monolayers [19]. Most studies focus on foam film and its elasticity, adsorption, and viscoelastic properties of the adsorption films. Therefore, determining the influence of hydrocarbon chain length on foam properties is important.

The foam properties of surfactant solutions were studied using the commercially available FoamScan instrument. To date, three main methods are used to measure foam properties, namely Ross–Miles, Winding, and FoamScan methods. Different foaming techniques were used to generate the foam, such as sparging or stirring (FoamScan method), pouring (standardized Ross–Miles test), and shaking (Winding test). The Ross–Miles method is often specifically used to measure foamability and foam stability of formulations in the industrial sector [20]; this method is restricted to dry foams as it produces quite airy foams [21]. The Winding method needs the same shaking rate, and the rotation rate, number, and direction of shaking will influence the results of the measurement.

FoamScan was used to generate foam by sparging gas at a fixed flow rate through a porous disc or by stirring the solution at the bottom. The foam and liquid volumes are measured by conductivity measurements. The images of the foams are recorded by two CCD cameras and analyzed with cell size analysis software [22, 23], which improves the accuracy of the experiment and avoids the errors made by observation with the naked eyes.

In the present work, the foam properties of alkyl polyglycosides (APGs) with different hydrocarbon chains were studied with FoamScan. This study investigated the influence of hydrocarbon chains on foam properties. The results provide useful information on the application of APGs with different hydrocarbon chains.

Experimental Procedures

Materials and Cleaning Procedure

Non-ionic sugar surfactant APGs with different hydrocarbon chains, C_6 APG, C_8 APG, $C_{8–10}$ APG, $C_{9–11}$ APG, and $C_{12–14}$ APG, were supplied by Sinolight Chemicals Co., Ltd. (P.R. China) and used directly without further purification; their active matter contents are 75, 60, 50, 50, and 50 wt%, respectively. Sodium chloride (NaCl, ≥99.8%) was obtained from Beijing Source Raw Chemical Co. Ltd. (P.R. China) and roasted at 500 °C for 24 h to drive off organic contaminants. The liquid content is determined via electrical conductivity; thus, a minimum electrolyte concentration of 0.15 wt% NaCl is required, and at this concentration, the presence of the electrolyte has no measurable influence on the foaming properties. All the surfactant solutions were prepared with doubly distilled water. All glassware was rinsed thoroughly with deionized water before use.

Measurement

The commercially available FoamScan (FoamScan IT Concept, Teclis Co., France) was used for conductivity measurements and image analysis to monitor the foaming properties. Foamability, foam stability, and drainage of liquids can be obtained. Bubble number and bubble size can be analyzed with cell size analysis.

The details of the FoamScan method were described in previous studies [20, 22, 24]. The measurement at hand was introduced briefly as follows: the foams were produced by sparging nitrogen through a porous glass disc (pore size of 14–16 μm and thickness of 3 mm) at the bottom of a square glass column (inside 25 mm); the volume of surfactant solution was fixed at 40 mL, which was divided into three and separately injected into the square glass. The first injection volume was 20 mL, and the other two injection volumes were 10 mL. The gas flow rate of 40 mL/min allowed a balance between foam generation and foam destruction during foaming. In all experiments, the time of blowing nitrogen we set at 120 s and then it was stopped automatically. The volume of foam V_{120} is considered as foamability. All measurements were performed with $T = 25 \pm 0.2$ °C.

Results and Discussion

Foamability

The procedures for the foam volume measurements of the five APGs as a function of time for various concentrations are exhibited in Fig. 1. The curves describe the foaming process and the decay of foam volume. The V_{120} values, which were taken after blowing foam for 120 s, are summarized in Fig. 2. V_{120} indicates the foaming capacity. As we can see in Figs. 1 and 2, the foaming volume of all surfactants increases with increasing surfactant concentration. The foaming volume of short-chain surfactant increases more rapidly compared to that of the long-chain surfactants. Among all the surfactant concentrations investigated, the V_{120} of C_6 APG was the shortest; however, $C_{12–14}$ APG has the highest V_{120} value and the rest were within the range of 80–86 mL. C_6 APG has worse foamability compared with the others, whereas $C_{12–14}$ has the best foamability. Foamability depends on two aspects: the total adsorbed amount of surfactants and the diffusion rate of surfactant molecules to water–air interface [25]. The observed differences among the surfactants can be explained as follows.

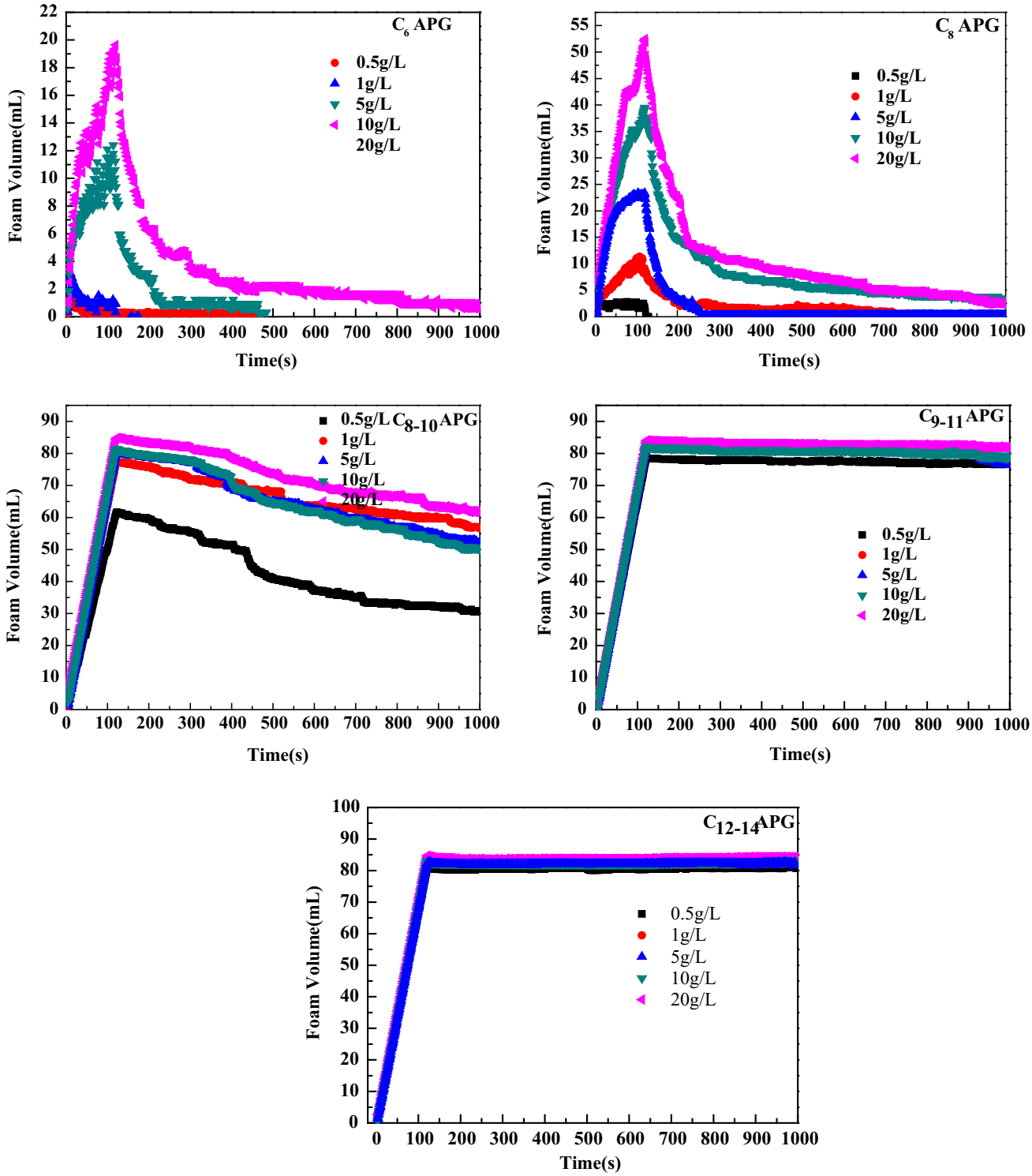

Fig. 1 Evolution of the foam volume of five APGs as a function of time

First, an increase in V_{120} with increasing surfactant concentration indicates an increase in the amount of the adsorbed surfactant. When the surfactant concentration of bulk solution is added gradually, more molecules are rapidly adsorbed from the bulk to the surface until surfactant adsorption reaches saturation. Thus, the film at the air–water surface is formed easily and more surface area is obtained, forming small bubbles [26]. Second, long-chain surfactants produce higher volumes of initial foam as compared with short-chain surfactants because of their

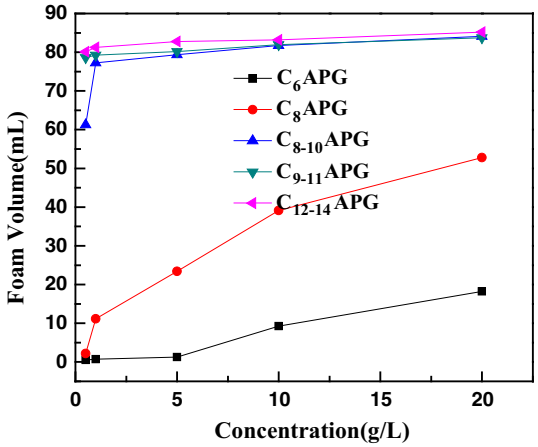

Fig. 2 Foamability as a function of surfactant concentration

effectiveness in reducing surface tension and in strengthening intermolecular cohesive force. On the contrary, the interface stringencies of C_6 APG and C_8 APG are weak because of their weak molecular cohesive force.

Foam Stability, Liquid Carrying Ability, and Drainage

Foam stability is usually represented by the foam volume decay time or the liquid volume in the foams. The variation of foam volumes is exhibited in Fig. 1, which shows that until 1000 s, the foam volume of $C_{9–11}$ APG and $C_{12–14}$ APG are slightly decreased and remain higher than that of the others. At 200 s, the foam volume of C_8 APG is less than half, whereas that of C_6 APG is almost zero. V_{1000} is the foam volume at 1000 s. Figure 3 shows the V_{1000} generated by different surfactants under different concentrations. The V_{1000} values of all surfactants increase with increasing surfactant concentration. The V_{1000} values of C_6 APG and C_8 APG are almost zero, whereas there was little change for $C_{9–11}$ APG and $C_{12–14}$ APG.

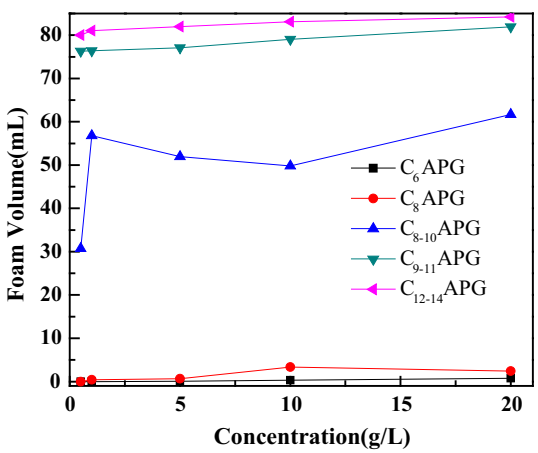

Fig. 3 Foam volume at 1000 s as a function of surfactant concentration

The variations in liquid volumes of the foams generated by five surfactants are exhibited in Fig. 4. All the liquid volume in the foams first increases and then decreases gradually as shown in Fig. 4; the longer hydrophobic chain surfactant is, the larger the liquid volume in the foam is; the maximum liquid volume in the foams of $C_{12–14}$ APG was about 1.53 mL, while that of C_6 APG was only 0.19 mL at a concentration of 20 g/L.

Foam drainage is extremely important for stability, and it is controlled by gravity and lamella pressure [27]. As a result of the influence of gravity, gravity drainage is carried out during the process of blowing, and the liquid in foams flows downward along the network. Gravity drainage is the main driving force until the blowing is stopped. At the beginning of stopping the blowing, gravity drainage is the main means of foam attenuation. As the water in foams becomes less and less, until the bubble becomes dry foam, the adsorption layer at the air–water interface foam is an additional phase which is considered as a critical effect for the stability of dry foam. The compactness of the surfactant monolayer in the interface decides the monolayer stringency [19].

Scheme 1 provides a sketch map describing the spatial configurations of the five surfactant molecules with different long hydrocarbon tails in the air–water interfacial layer. The interfacial layer molecular packing density is closer with an increase in the hydrophobic chains. The gas diffusion between adjacent bubbles gradually decreased because of the denser air–water interfacial layer. In addition, the long alkyl chain of APG has strong cohesion and its alkyl chain is easily cross-linked and entangled, which increases interfacial layer ductility and strength. Therefore, the long-chain APG forms more stable foam than short-chain APG.

Foam Morphology

C_6 APG and C_8 APG have low foaming volumes, which were observed in the corresponding images after 200 s. The bubble change processes generated from 20 g/L $C_{8–10}$ APG, $C_{9–11}$ APG, and $C_{12–14}$ APG solution were measured and analyzed. The bubble change processes of the three surfactants were roughly the same. The bubble images of $C_{12–14}$ APG are shown in Fig. 5. Table 1 shows the results for the three surfactants.

As shown in Fig. 5, the shape of foam gradually changes from spherical to polyhedral, which is consistent with the results of Barik and Roy [28]. The color of the air–water interfacial layer gradually changed from dark to light as the liquid is lost. The foam number, defined as the number of intact bubbles in the photo, gradually decreases and the

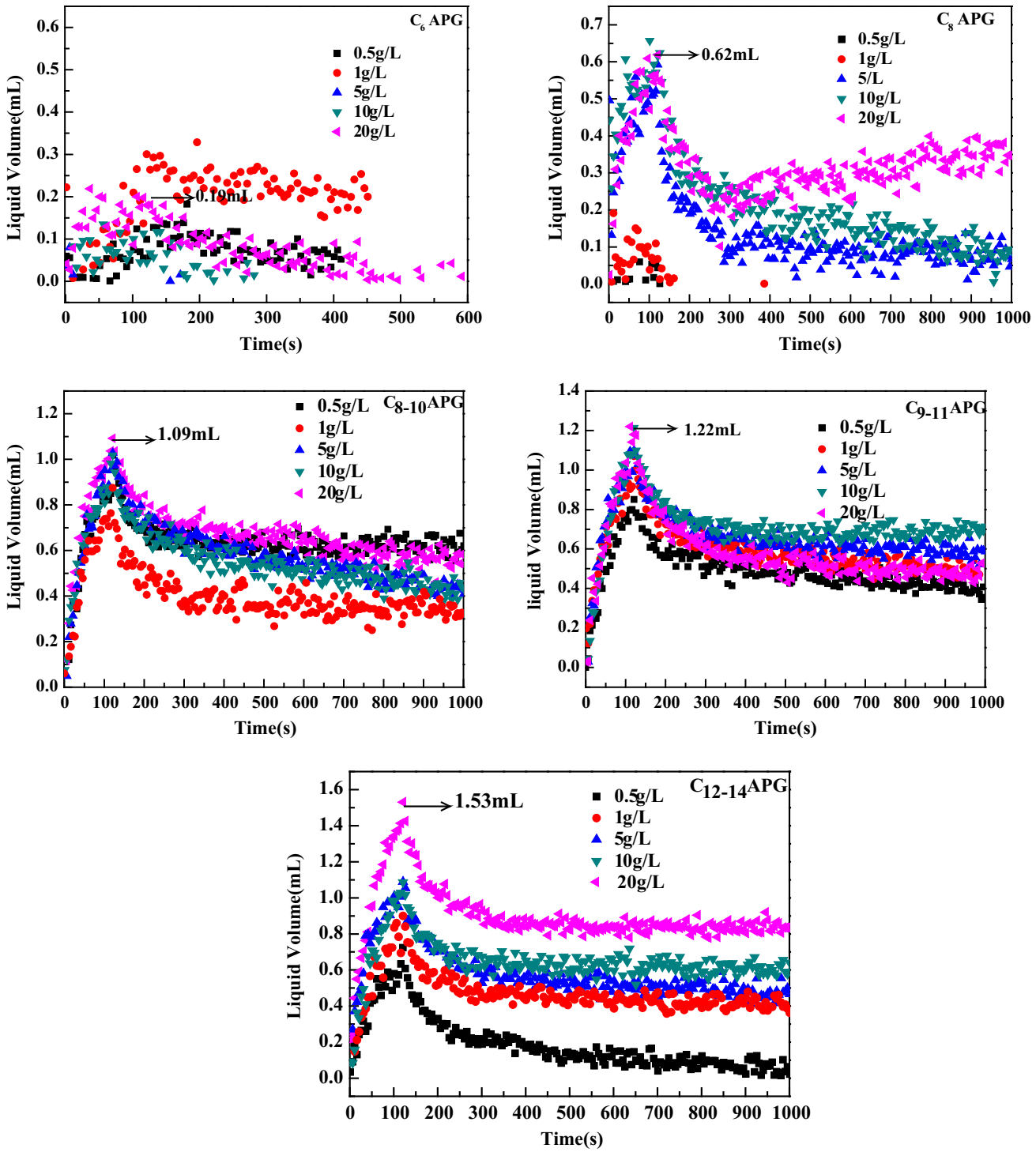

Fig. 4 Liquid volume in the foams as a function of time

average area increases, as can be seen from Table 1. Initially, $C_{8–10}$ APG was abundant, with the largest foam number, but disappeared at 1000 s. The change of average area of $C_{12–14}$ APG was only from 0.45 to 0.69 mm^2, whereas that of $C_{8–10}$ APG was from 0.33 to 0 mm^2, which indicates that the rate of drainage, collapse, and coalescence of $C_{8–10}$ APG is faster than that of $C_{12–14}$ APG. This finding also illustrates that foam stability of $C_{12–14}$ APG is better than that of $C_{8–10}$ APG. This occurrence can be attributed to the diffusion of gas from small to large bubbles, which, by the Laplace–Young law, contributes to the coarsening of the bubble. The smaller

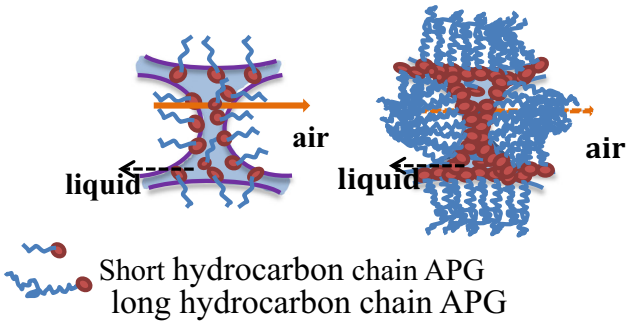

Scheme 1 Schematic illustration of molecular arrangement at the air–water interface for different hydrocarbon chain APGs

bubbles are gradually eliminated (as seen in Fig. 5) and the large bubbles become larger [29]. Gravity and capillarity pressure are the driving forces that make the liquid drain out along the interfacial layer and plateau borders. The process stops when gravity and the capillarity pressure reach equilibrium. Eventually, the adjacent bubbles coalesce [30], and the average area of bubbles increases with decreasing of foam numbers.

The number and average area of foams generated by five APGs in different concentration solutions at 350 s were obtained, and the data are displayed in Table 2. As shown in Fig. 4, the residual liquid volume in the foams is very

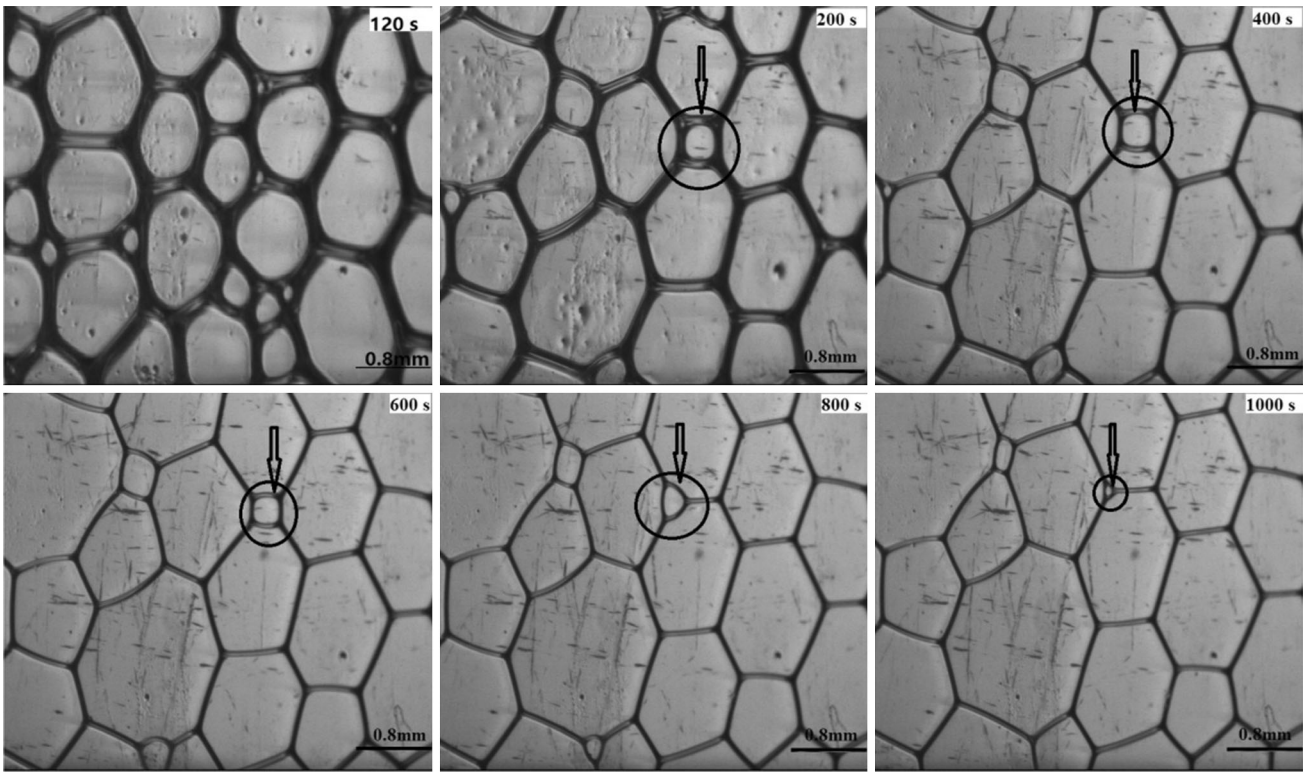

Fig. 5 Variation of the foams generated from 20 g/L $C_{12–14}$ APG as a function of time

Table 1 Number and average area of foams generated by five APG at different times

Time (s)	Foam number			Foam area (mm^2)			Average area (mm^2)		
	$C_{8–10}$ APG	$C_{9–11}$ APG	$C_{12–14}$ APG	$C_{8–10}$ APG	$C_{9–11}$ APG	$C_{12–14}$ APG	$C_{8–10}$ APG	$C_{9–11}$ APG	$C_{12–14}$ APG
200	83	72	61	27.10	26.27	27.17	0.33	0.37	0.45
400	28	59	54	32.37	28.48	30.81	0.55	0.48	0.57
500	56	57	55	32.46	28.96	31.68	0.58	0.51	0.57
600	48	45	47	32.56	29.84	31.87	0.68	0.66	0.68
800	40	38	50	35.64	28.50	32.52	0.89	0.75	0.65
1000	0	10	47	0	8.00	32.43	0	0.80	0.69

Table 2 Number and average area of foams generated by five APGs at different concentrations at 350 s

Concentration (g/L)	Foam number			Foam area (mm^2)			Average area (mm^2)		
	$C_{8–10}$ APG	$C_{9–11}$ APG	$C_{12–14}$ APG	$C_{8–10}$ APG	$C_{9–11}$ APG	$C_{12–14}$ APG	$C_{8–10}$ APG	$C_{9–11}$ APG	$C_{12–14}$ APG
0.5	73	54	77	32.10	32.34	29.20	0.44	0.54	0.38
1	45	59	79	33.59	33.19	28.31	0.75	0.48	0.31
5	43	77	78	32.34	30.33	28.95	0.75	0.39	0.37
10	40	86	82	32.61	29.36	29.04	0.82	0.34	0.35
20	38	67	80	31.59	28.14	30.15	0.83	0.42	0.38

low at 350 s, during which drainage becomes very slow and foam stability is dominated by Ostwald ripening and bubble merging processes. The same result showed that the average area of $C_{8–10}$ APG foams increases with increasing the surfactant concentration, whereas that of $C_{9–11}$ APG and $C_{12–14}$ APG did not change a lot. This result can be explained as follows: though the adsorption quantity of $C_{8–10}$ APG increases with an increase in bulk concentration and can lead to a closer packing of the surfactant molecules in the film to some extent, it cannot, however, decrease the rate of diffusion of the gas between bubbles. Thus, the average area of the $C_{8–10}$ APG bubbles increases with increasing surfactant concentration. Because of their strong cohesion and ductility, the Ostwald ripening and bubble merging processes of the long alkyl chain of $C_{9–11}$ APG and $C_{12–14}$ APG are not severe, and they show more stable foam than the APG with short hydrophobic chain.

Conclusion

The foam properties are very important for surfactants which are widely used in a variety of applications. The influence of the hydrophobic length of alkyl polyglycosides (APGs) on foam properties has been investigated. The foaming volumes of aqueous solutions of all surfactants increase with increasing surfactant concentrations. Foamability, foam stability, and the liquid carrying ability increase with increasing hydrophobic length of the surfactant. This is attributed to the total adsorbed amount of surfactants and the diffusion rate of surfactant molecules to the water–air interface.

As the time increases, aqueous solutions of the five APGs studied show similar tendencies. The shape of foam gradually changes from spherical to polyhedral, and the foam number gradually decreases with the average area increase. The difference in the hydrophobic length of surfactants affects the interfacial layer molecular packing density, cohesion, interfacial layer ductility, and strength, which then affect the foam properties.

Acknowledgements We gratefully acknowledge the financial support of the National Natural Science Foundation of China (21203005, 21677003), the National Key Technologies Research and Development Program of China during the 12th Five-Year Plan (No. 2014BAE03B01), the Science and Technology Program Key Project of Beijing Municipal Commission of Education (KZ201510011010), and the Transformation of Scientific and Technological Achievements-Promotion Plan Project (TJSHG201510011020).

References

1. Exerowa D, Kruglyakov PM. Foam and foam films: theory, experiment, application. Amsterdam: Elsevier; 1997.
2. Stubenrauch C, Shrestha LK, Varade D, et al. Aqueous foams stabilized by *n*-dodecyl-β-D-maltoside, hexaethyleneglycol monododecyl ether, and their 1:1 mixture. Soft Matter. 2009;5:3070–80.
3. Weaure D, Hutzler S. The physics of foams. London: Oxford University Press; 2000.
4. Wang J, Nguyen AV, Farrokhpay S. A critical review of the growth, drainage and collapse of foams. Adv Colloid Interface Sci. 2016;228:55–70.
5. Schelero N, Hedicke G, Linse P. Effects of countries and co-ions on foam films stabilized by anionic dodecyl sulfate. J Phys Chem B. 2010;114:15523–9.
6. Wu X, Zhao J, Li E. Interfacial dilational viscoelasticity and foam stability in quaternary ammonium gemini surfactant systems: influence of intermolecular hydrogen bonding. Colloid Polym Sci. 2011;289:1025–34.
7. Wang J, Liu H, Ning Z. Experimental research and quantitative characterization of nitrogen foam blocking characteristics. Energy Fuels. 2012;26:5152–63.
8. Pradines V, Fainerman VB, Aksenenko EV. Miller, adsorption of protein–surfactant complexes at the water/oil interface. Langmuir. 2010;27:965–71.
9. Carey E, Stubenrauch C. Foaming properties of mixtures of a non-ionic (C_{12} DMPO) and an ionic surfactant (C_{12} TAB). J Colloid Interface Sci. 2010;346:414–23.
10. Hu X, Li Y, He X. Structure–behavior–property relationship study of surfactants as foam stabilizers explored by experimental and molecular simulation approaches. J Phys Chem B. 2011;116:160–7.
11. Stubenrauch C, Rippner-blomqvist B. Colloid stability: the role of surface forces, part 1. In: Tadros T, editor. Colloid and interface science series. Weinheim: Wiley-VCH; 2006.
12. Beneventi D, Carre B, Gandini A. Role of surfactant structure on surface and foaming properties. Colloid Surf A. 2001;189:65–73.

13. Stubenrauch C, Khristov K. Foams and foam films stabilized by C_nTAB: influence of the chain length and of impurities. J Colloid Interface Sci. 2005;286:710–8.
14. Tehrani-bagha AR, Holmberg K. Cationic ester-containing gemini surfactants: physical–chemical properties. Langmuir. 2010;26:9276–82.
15. You Y, Wu X, Zhao J. Effect of alkyl tail length of quaternary ammonium gemini surfactants on foaming properties. Colloid Surf A. 2011;384:164–71.
16. Tan SN, Fornasiero D, Sedev R. The role of surfactant structure on foam behavior. Colloid Surf A. 2005;263:233–8.
17. Tamura T, Takeuchi Y, Kaneko Y. Influence of surfactant structure on the drainage of nonionic surfactant foam films. Colloid Surf A. 1998;206:112–21.
18. Wang XC, Zhang L, Gong QT. Study on foaming properties and dynamic surface tension of sodium branched-alkyl benzene sulfonates. J Dispers Sci Technol. 2009;30:137–43.
19. Wang XC, Zhang L, Gong QT. A study of dynamic interfacial properties as related to foaming properties of 2,5-dialkyl benzene sulfonates. J Dispers Sci Technol. 2009;30:346–52.
20. Carey E, Stubenrauch C. Properties of aqueous foams stabilized by dodecyltrimethylammonium bromide. J Colloid Interface Sci. 2009;333:619–27.
21. Lunkenheimer K, Malysa K. A simple automated method of quantitative characterization of foam behaviour. Polym Int. 2003;52:536–47.
22. Ropers MH, Novales B, Boué F. Polysaccharide/surfactant complexes at the air–water interface—effect of the charge density on interfacial and foaming behaviors. Langmuir. 2008;24:12849–57.
23. Rami-Shojaei S, Vachier C, Schmitt C. Automatic analysis of 2D foam sequences: application to the characterization of aqueous proteins foams stability. Image Vis Comput. 2009;27:609–22.
24. Care E, Stubenrauch C. A disjoining pressure study of foam films stabilized by mixtures of nonionic (C_{12} DMPO) and an ionic surfactant (C_{12} TAB). J Colloid Interface Sci. 2010;343:314–23.
25. Pugh RJ. Foaming, foam films, antifoaming and defoaming. Adv Colloid Interface Sci. 1996;64:67–142.
26. Zhang H, Xu G, Liu T. Foam and interfacial properties of Tween 20–bovine serum albumin systems. Colloid Surf A. 2013;416:23–31.
27. Rosen MJ, Kunjappu JT. Surfactants and interfacial phenomena. 4th ed. New York: Wiley; 2012.
28. Barik TK, Roy A. Statistical distribution of bubble size in wet foam. Chem Eng Sci. 2009;64:2039–43.
29. Julia B, Wiebke D, Cosima S. Protocol for studying aqueous foams stabilized by surfactant mixtures. J Surfact Deterg. 2013;16:1–12.
30. Weaire D, Hutzler S. Nonlinear phenomena in soap froth. Phys A Mech Appl. 1998;257:264–74.

Yawen Zhou received an M.S. in applied chemistry from the China Research Institute of Daily Chemical Industry. She is an associate professor whose research focuses on the synthesis and properties of surfactants.

Shan Wang is a postgraduate student in applied chemistry at Beijing Technology and Business University. His main research field is the properties and applications of surfactants.

Mengdie Lv is a postgraduate student in applied chemistry at Beijing Technology and Business University. Her research interests are the synthesis and properties of surfactants.

Jinping Niu was born in 1966. Her research interests are the sulfonation/sulfation of organic materials and application of surfactants for EOR.

Baocai Xu received a Ph.D. in applied chemistry from Beijing Institute of Technology. He is a professor at Beijing Key Laboratory of Flavor Chemistry, Beijing Higher Institution Engineering Research Center of Food Additives and Ingredients. His research focuses on the synthesis and properties of surfactants.